

## Article

# Adjustment of Subwavelength Rippled Structures on Titanium by Two-Step Fabrication Using Femtosecond Laser Pulses

Yanping Yuan <sup>1,2,3,\*</sup>, Xinyang Guo <sup>1,2,3</sup>, Yitong Shang <sup>4</sup> and Jimin Chen <sup>1,2,3</sup>

<sup>1</sup> Faculty of Materials and Manufacturing, Beijing University of Technology, Beijing 100124, China; xinyangguo@mails.bjut.edu.cn (X.G.); jimin@bjut.edu.cn (J.C.)

<sup>2</sup> Beijing Engineering Research Center of 3D Printing for Digital Medical Health, Beijing University of Technology, Beijing 100124, China

<sup>3</sup> Key Laboratory of Trans-Scale Laser Manufacturing Technology (Beijing University of Technology), Ministry of Education, Beijing 100124, China

<sup>4</sup> Beijing Institute of 3D Printing, Beijing City University, Beijing 100083, China; yt\_shang@126.com

\* Correspondence: ypyuan@bjut.edu.cn

**Abstract:** An effective approach is proposed to adjust the surface morphology induced by using a femtosecond laser, including the area and period of rippled structures. The effect of the processing steps and laser polarization on the surface morphology of rippled structures on a titanium surface was experimentally investigated in this study. A processing sequence was designed for two series of femtosecond laser pulses that irradiate a titanium surface, for example,  $N = 50(0^\circ) + 50(90^\circ)$ . The experimental results show that the area and period of rippled structures can be simultaneously adjusted by following a two-step method. Due to the enhancement of energy absorption and SP-laser coupling of the initial rippled structures, large area surface structures with small periods are fabricated using two series of femtosecond laser pulses with the same polarization direction. By changing the polarization direction of the two series of femtosecond laser pulses, the recording, erasing, and rewriting of subwavelength ripples is achieved. During the rewriting process, material removal and the formation of new ripples simultaneously occur.

**Keywords:** surface morphology; subwavelength ripples; femtosecond laser; two-step method



**Citation:** Yuan, Y.; Guo, X.; Shang, Y.; Chen, J. Adjustment of Subwavelength Rippled Structures on Titanium by Two-Step Fabrication Using Femtosecond Laser Pulses. *Appl. Sci.* **2021**, *11*, 2250. <https://doi.org/10.3390/app11052250>

Academic Editor: Giulio Nicola Cerullo

Received: 17 January 2021  
Accepted: 26 February 2021  
Published: 4 March 2021

**Publisher's Note:** MDPI stays neutral with regard to jurisdictional claims in published maps and institutional affiliations.



**Copyright:** © 2021 by the authors. Licensee MDPI, Basel, Switzerland. This article is an open access article distributed under the terms and conditions of the Creative Commons Attribution (CC BY) license (<https://creativecommons.org/licenses/by/4.0/>).

## 1. Introduction

Surface morphology is a key factor associated with changes and the control of surface properties of a solid such as mechanical, optical, biological, and chemical properties. Fabricating micro-nano structures is one of the main methods for changing surface morphology [1]. Laser-induced periodic surface structures (LIPSS, also referred to as ripples) are a simple and rapid method of fabricating micro-nano surface structures, when the incident fluence is slightly higher than the ablation threshold of the material [2–6]. Due to the superior ability to control the surface properties, ripples have been widely used in many fields, including optics [7], optoelectronics [8], micro-nano fluids [9], biomedicine [10–13] and biological implants [14–19]. Regarding applications of biological implants, studies have shown that the growth of cells is selective to the surface morphology of materials [14–24]. Generally, cells tend to grow along grooves on the surface, and the degree of this trend depends on the depth and width of the groove on the surface. In addition, different cells have different requirements for the surface morphology of an implant. For example, fibroblasts are more oriented on the surface grooves. Hence, it is essential to adjust and control the periodic surface structure.

When the incident fluence is slightly higher than the ablation threshold, ripple structures can be observed in various materials, including metals [6,25], semiconductors [26,27], and dielectrics [28–30]. The rippled structure can be divided into two types, i.e., typical ripples and subwavelength ripples. Due to interference between incident laser and surface-scattered waves [31,32], ripples with the periods close to the wavelength of the incident

laser (known as typical ripples) are induced by the laser. With the development of lasers, various new types of ripples have been observed experimentally, with the characteristic of being significantly smaller than the incident wavelength (known as subwavelength ripples). In order to better adjust subwavelength rippled structures, relevant theoretical and experimental studies have been carried out. Many studies have reported on the formation mechanisms of subwavelength ripples, including self-organization [33,34], second harmonic generation [35], Coulomb explosion [36], and interaction between the incident laser and surface plasmon [37–39]. However, the interaction between the laser and material is a nonlinear and nonequilibrium dynamic process, which causes some differences between theoretical research and experimental results. In addition, many factors significantly affect the formation and morphology of ripples [30,40–49], such as wavelength, pulse duration, number of pulses, pulse fluence, polarization, incidence angle, repetition rate, pulse delay, number of pulse trains, spatial distribution of laser energy, processing environment, processing mode, and processing materials. For the aforementioned application of ripple structures, it is still a significant challenge to efficiently fabricate uniform rippled structures with a large area. During the fabrication of uniform rippled structures with a large area, the scanning speed and the scanning interval are crucial for the surface morphologies of the rippled structures [50]. However, there is still a lack of methods for synthetically regulating the area and period of rippled structures fabricated using a femtosecond laser.

In order to adjust the area and period of rippled structures induced by a femtosecond laser, the effects of the processing steps and laser polarization on the surface morphology of rippled structures on a titanium surface are experimentally investigated in this study. The processing sequence is designed, and two series of femtosecond laser pulses irradiate the titanium surface, for example,  $N = 50(0^\circ) + 50(90^\circ)$ . The experimental results show that the area and period of the rippled structures can be simultaneously adjusted by following a two-step method. Large area surface structures with small periods can be fabricated using two series of a femtosecond laser with the same polarization direction, because the existing ripples induced by the first series of femtosecond laser can strongly enhance the energy absorption and SP-laser coupling. The recording, erasing and rewriting of subwavelength ripples can be achieved by changing the polarization direction of the two series of femtosecond laser pulses. The experimental results indicate that a two-step method is an effective method to control the surface morphology in order to better fabricate large-area, uniform ripple structures.

## 2. Materials and Methods

In our experiments, we used a femtosecond Ti-sapphire laser system (Spectra-Physics, Santa Clara, CA, United States) to generate a laser pulse with a central wavelength of 800 nm, pulse width of 50 fs, and a repetition rate of 100 Hz. A half-wave plate and a mechanical shutter were used to control the polarization direction and the pulse number, respectively. The laser beam was normally focused on the surface of the sample by using a dichroic mirror and lens with an achromatic doublet ( $f = 100$  mm). A beam radius of  $w_0 (1/e^2) \sim 40 \mu\text{m}$  was determined in the processing plane. The incident laser was focused on the surface of pure titanium samples ( $10 \times 10 \times 0.5$  mm, Kejing Hefei). The incident laser fluence was fixed at  $0.20 \text{ J/cm}^2$ , which is slightly higher than the ablation threshold of titanium,  $0.16 \text{ J/cm}^2$ . The experiments were performed at room temperature. All the processing was monitored using a CCD camera (Basler, Ahrensburg, Germany). Following the femtosecond laser ablation, a scanning electron microscope (SEM) (SEM-FEG XL30, FEI, Hillsboro, OR, USA) was used to characterize the surface morphologies of the titanium samples.

## 3. Results

In order to adjust the area and period of rippled structures induced by using a femtosecond laser, the effects of the processing steps on the area and period of rippled structures on a titanium surface are experimentally investigated in this study. For the experiments,

the total number of pulses ( $N$ ) is fixed at 100 and the incident fluence is about  $0.20 \text{ J/cm}^2$ . In order to study the effect of two-step processing on surface morphology, the following three processing sequences are designed:  $N = 100$ ,  $N = 40 + 60$ , and  $N = 60 + 40$ . For example,  $N = 100$  represents 100 pulses to induce the surface micro-nano structure in one step.  $N = 40 + 60$  represents two series of femtosecond laser pulses to irradiate the titanium surface. The first series consists of 40 pulses, and the second series consists of 60 pulses. The time interval between the two series is a few seconds to tens of seconds. This process is called a two-step method. Figure 1 shows the SEM images of ablation morphology and subwavelength ripples on titanium obtained following the two-step fabrication method. The areas circled in orange represent regions with surface rippled structures, as shown in Figure 1a,c,e. The size of the area circled in orange is represented by its diameter,  $D$ . The diameters of the areas circled in orange are about  $18.9 \pm 0.1$ ,  $20.0 \pm 0.08$ , and  $21.9 \pm 0.05 \mu\text{m}$  under the processing sequences  $N = 100$ ,  $N = 40 + 60$ , and  $N = 60 + 40$ , respectively. As shown in Figure 1b,d,f, the periods of ripples with a perpendicular oriented laser polarization are in the range of  $480 \pm 20 \text{ nm}$ ,  $465 \pm 20 \text{ nm}$ , and  $430 \pm 30 \text{ nm}$  for the processing sequences  $N = 100$ ,  $N = 40 + 60$ , and  $N = 60 + 40$ , respectively. Similar rippled structures have also been reported in [22]. The experimental results show that the areas of rippled structures induced by using a femtosecond laser can be effectively increased following a two-step fabrication method. The periods of ripples formed on the titanium surface have also been effectively adjusted by the designed processing sequence. The experimental results indicate that it is possible to fabricate large area surface structures with small periods following a two-step method.

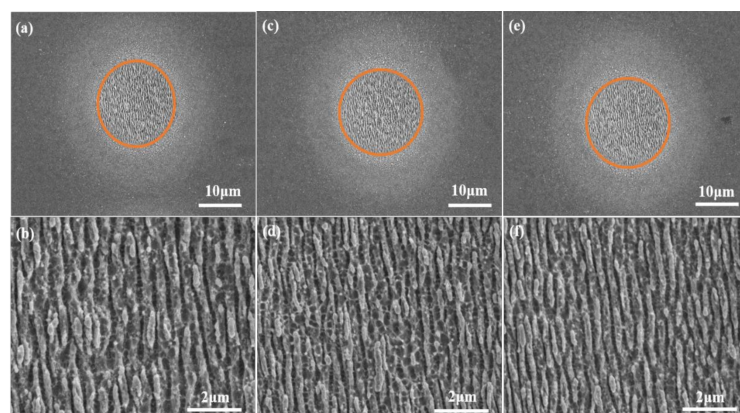


**Figure 1.** SEM images of ablation morphology and subwavelength ripples on titanium obtained by one- and two-step fabrication. (a,b)  $N = 100$ ; (c,d)  $N = 40 + 60$ . (e,f)  $N = 60 + 40$ .

For the processing sequences  $N = 40 + 60$  and  $N = 60 + 40$ , the formation of rippled structures induced following a two-step method can be divided into two processes: rippled structures induced by the first series pulses (the first process) and rippled structures induced by second series pulses (the second process). For the first process ( $N = 40 + 60$ ), the initial surface plasmon (SP)-laser interference plays an important role, based on our previous study [37]. At the interface between a metal with permittivity  $\epsilon_M$  and air with permittivity  $\epsilon_A$ , if the value of the real component of the complex dielectric function is less than  $-1$ , surface plasmons can be resonantly excited by the coupling between the surface electrons of the dielectric and the incident field, which is characterized by surface electromagnetic waves (also called the surface plasmon field). For metals, the excitation conditions of the surface plasma field are always satisfied after the incident femtosecond laser irradiation. Because of the interference between the absorbed laser field and the surface plasmon field, the coupling field intensity is enhanced in some areas and reduced in other areas. The absorbed laser beam profile is reshaped by the presence of surface plasmons, which displays periodic patterns. Then, energy with spatially periodic patterns leads to the periodic patterns of the free electron temperature distribution and lattice

temperature distribution. Due to the interactions of laser and materials, subwavelength ripples are formed in some areas. For the second process ( $N = 60 + 40$ ), the initial rippled structures induced by the first series of pulses are equivalent to the preset grating structures in our previous study [30]. The existing ripples can significantly enhance the energy absorption and the SP-laser coupling, and the SP-laser coupling intensities are much more intense in the grooves, which makes the fabrication of subwavelength ripples more efficient [30].

In order to investigate the detailed effects of the processing steps on the area and period of rippled structures, a series of experiments are designed as shown in Figure 2a–c. Polarization of an incident laser is a key factor associated with the formation of subwavelength ripples. Hence, the effects of laser polarization on the area and period of rippled structures on a titanium surface are experimentally investigated in this study. Figure 2 shows the illustrated process of the experiments. Subwavelength ripples are induced by  $2N$  femtosecond laser pulses on the surface of the sample, as shown in Figure 2a, which is denoted by  $2N(0^\circ)$ , where  $N$  is the number of incident laser pulses and  $0^\circ$  means the laser polarization rotated  $0^\circ$  with respect to the original polarization. Then, we apply two series of femtosecond laser pulses to irradiate the same place on the sample surface, as shown in Figure 2b. First, the titanium sample is irradiated by the first series of femtosecond laser pulses, and then by a second series of femtosecond laser pulses on the same place. For example, the laser processing shown in Figure 2b is denoted by  $N(0^\circ) + N(0^\circ)$ . In order to investigate the change of rippled structures, the second series of pulses with the laser polarization rotated  $90^\circ$  with respect to the original polarization are used to irradiate the same place on the sample surface, as shown in Figure 2c, which is denoted by  $N(0^\circ) + N(90^\circ)$ . Figure 2d–f are the corresponding experimental results of Figure 2a,b. The experimental results shown in Figure 2d,e indicate the effects of pulse number on the area and period of rippled structures on the titanium surface, which is attributed to the incubation effects during the multi-shot regime [6]. As shown in Figure 2e,f, the polarization of a femtosecond laser significantly affects the surface topography, especially the direction of the rippled structure. Figure 2e,f show the processing of recording, erasing, and rewriting of subwavelength ripples induced by the femtosecond laser.

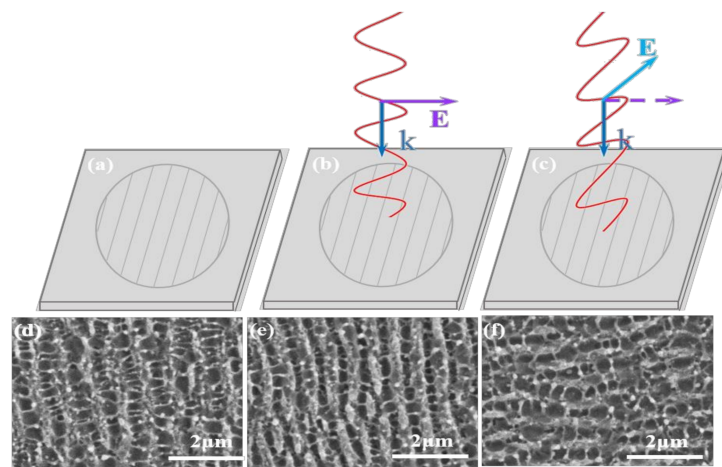


**Figure 2.** Schematic of experimental processing of ripples on a titanium surface. (a) Subwavelength ripples induced using a  $2N$  femtosecond laser pulses; (b) Subwavelength ripples induced using two series of femtosecond laser pulses, denoted by  $N(0^\circ) + N(0^\circ)$ ; (c) Subwavelength ripples induced using two series of femtosecond laser pulses, denoted by  $N(0^\circ) + N(90^\circ)$ ; (d–f) are the corresponding experimental results of (a–c).

The detailed SEM images of the ablation morphology and subwavelength ripples on titanium obtained by following a two-step method for femtosecond laser fabrication are shown in Figure 3. The diameters of rippled regions are about  $20.8 \pm 0.06$  and

$19.6 \pm 0.09 \mu\text{m}$  under the conditions  $50(0^\circ) + 50(0^\circ)$  and  $50(0^\circ) + 50(90^\circ)$ , respectively. The periods of subwavelength ripples are in the range of  $450 \pm 25 \text{ nm}$  to  $560 \pm 15 \text{ nm}$  under the conditions  $50(0^\circ) + 50(0^\circ)$  and  $50(0^\circ) + 50(90^\circ)$ , respectively. By comparing with the experimental results shown in Figure 1a, it can easily be observed that the diameters of rippled regions under the conditions  $N = 50(0^\circ) + 50(0^\circ)$  and  $N = 50(0^\circ) + 50(90^\circ)$  are much larger than the diameter under the condition of  $N = 100(0^\circ)$ . This phenomenon is caused by the incubation effect due to the accumulation of laser-induced structural changes of the material during the femtosecond laser ablation. The existing rippled structure can improve absorption efficiency [6]. The period of subwavelength ripples under the condition  $N = 50(0^\circ) + 50(0^\circ)$  is much smaller than the periods under the condition of  $N = 100(0^\circ)$ . According to our previous study [30], after the first series of femtosecond laser pulse irradiation, the initial rippled structures are formed on the surface of the titanium. The existing ripples can strongly enhance the energy absorption of the second series of femtosecond laser pulses and the enhanced laser intensity is mainly localized in the grooves. When the polarization is perpendicular to the already existing ripples, the second series of laser pulses can further deepen the grooves, thus, accelerating the ripple forming process [30]. For the condition  $N = 50(0^\circ) + 50(90^\circ)$ , the periods of the subwavelength ripples are larger than the periods under the condition  $N = 100(0^\circ)$  and the orientation of ripples is perpendicular to the polarization direction of the second series of femtosecond pulses. As shown in Figure 3e,f, the period of the rippled region under the condition  $N = 50(0^\circ) + 50(90^\circ)$  is similar to that induced by  $N = 50(0^\circ)$  (period in the range of  $550 \pm 15 \text{ nm}$ ) femtosecond laser pulses, which shows the processing of recording, erasing, and rewriting of ripples during femtosecond laser induced subwavelength ripples. Similar phenomena have also been reported by [41]. During the rewriting process, when the number of pulses in the second sequence reach a certain number, the original ripples disappear. At the same time, the new ripples are already formed with an orientation of  $90^\circ$  to the original one, which means that two processes, including material removal and the formation of new ripples, simultaneously occur. Hence, as shown in Figure 3, we can easily observe the following: (1) the area and period of subwavelength rippled structures can be simultaneously adjusted by changing the processing sequence; (2) the area of rippled structure can be increased and its period can be decreased by two series of femtosecond laser pulses with the same polarization; (3) the recording, erasing, and rewriting of subwavelength ripples can be achieved using two series of femtosecond laser pulses with perpendicular polarization directions; (4) the period of subwavelength ripples under the condition  $50(0^\circ) + 50(90^\circ)$  is similar to that induced by  $N = 50(0^\circ)$  femtosecond laser pulses.

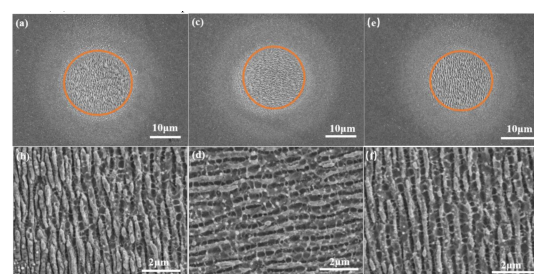


**Figure 3.** SEM images of ablation morphology and subwavelength ripples on titanium obtained by following one- and two-step fabrication processes. (a, b)  $N = 50(0^\circ) + 50(0^\circ)$ ; (c, d)  $N = 50(0^\circ) + 50(90^\circ)$ ; (e, f)  $N = 50(0^\circ)$ .

The subwavelength rippled structures are fabricated by following the two-step method using relatively fewer femtosecond laser pulses. The SEM images of ablation morphology and subwavelength ripples on titanium obtained at different femtosecond laser pulse irradiations are shown in Figure 4. The incident of the femtosecond laser is designed as follows:  $N = 20(0^\circ)$ ,  $N = 10(0^\circ) + 10(0^\circ)$ ,  $N = 10(0^\circ) + 10(90^\circ)$ , and  $N = 10(0^\circ)$ . The diameters of subwavelength rippled structures induced using the four femtosecond laser

designs are about  $14.8 \pm 0.16$ ,  $15.0 \pm 0.15$ ,  $13.6 \pm 0.22$ , and  $14.0 \pm 0.2 \mu\text{m}$ , respectively. The corresponding periods of the subwavelength ripples induced using the four femtosecond laser designs are  $590 \pm 15$ ,  $570 \pm 15$ ,  $620 \pm 10$ , and  $620 \pm 10 \text{ nm}$ , respectively. For a total of 20 pulses, the experimental results are highly similar to the situation of 100 pulses, which verifies the effectiveness of a two-step method in surface morphology.

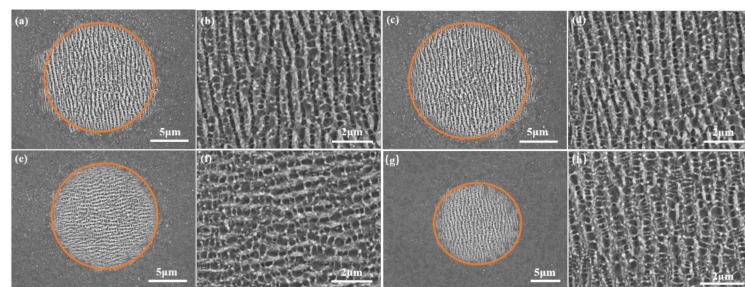


**Figure 4.** SEM images of ablation morphology and subwavelength ripples on titanium obtained at different femtosecond laser pulse irradiations. (a, b)  $N = 20$  ( $0^\circ$ ); (c, d)  $N = 10(0^\circ) + 10(0^\circ)$ ; (e, f)  $N = 10(0^\circ) + 10(90^\circ)$ ; (g, h)  $N = 10(0^\circ)$ .

#### 4. Conclusions

This study proposes an effective approach to control the surface morphology, including the area and period of rippled structures. The adjustment about the area and period of rippled structures induced using a femtosecond laser can be achieved by changing the processing steps and laser polarization. In order to fabricate the desired rippled structures, a series of experiments are designed, for example,  $N = 50(0^\circ) + 50(90^\circ)$  femtosecond laser irradiating the titanium surface. The experimental results show that the area and period of subwavelength rippled structures can be simultaneously adjusted by following a two-step method. Due to the enhancement of the energy absorption and SP-laser coupling by the initial rippled structures, large area surface structures with small periods can be fabricated by following a two-step method with the same polarization direction. The recording, erasing, and rewriting of subwavelength ripples can be achieved by using two series of femtosecond laser pulses with perpendicular polarization directions. During the rewriting process, material removal and the formation of new ripples simultaneously occur. This study has demonstrated the potential of following a two-step method to control the surface morphology of rippled structures that may have potential for titanium modification in orthopaedic or dental implant applications.

**Author Contributions:** Y.Y., X.G., and Y.S. designed the experiments, performed the SEM characterization and analyzed the data; Y.Y. wrote the manuscript; X.G. and Y.S. edited the manuscript; J.C. supervised the work. All authors have read and agreed to the published version of the manuscript.

**Funding:** This research was funded by the National Key R&D Program of China (grant no. 2018 YFB1107401), the National Natural Science Foundation of China (NSFC) (grant no. 51805014), the Research Foundation from Ministry of Education of China (6141A02033123), and the Scientific Research Program of Beijing Municipal Education Commission (grant no. KM201810005012).

**Institutional Review Board Statement:** Not applicable.

**Informed Consent Statement:** Not applicable.

**Data Availability Statement:** Data sharing not applicable.

**Conflicts of Interest:** The authors declare no conflict of interest.

## References

- Vorobyev, A.Y.; Guo, C. Direct femtosecond laser surface nano/microstructuring and its applications. *Laser Photonics Rev.* **2013**, *7*, 385–407. [[CrossRef](#)]
- Ding, S.; Zhu, D.; Xue, W.; Liu, W.; Cao, Y. Picosecond Laser-Induced Hierarchical Periodic Near-and Deep-Subwavelength Ripples on Stainless-Steel Surfaces. *Nanomaterials* **2020**, *10*, 62. [[CrossRef](#)] [[PubMed](#)]
- Ehrhardt, M.; Han, B.; Frost, F.; Lorenz, P.; Zimmer, K. Generation of laser-induced periodic surface structures (LIPSS) in fused silica by single NIR nanosecond laser pulse irradiation in confinement. *Appl. Surf. Sci.* **2019**, *470*, 56–62. [[CrossRef](#)]
- Chang, C.-L.; Cheng, C.-W.; Chen, J.-K. Femtosecond laser-induced periodic surface structures of copper: Experimental and modeling comparison. *Appl. Surf. Sci.* **2019**, *469*, 904–910. [[CrossRef](#)]
- Miyagawa, R.; Ohno, Y.; Deura, M.; Yonenaga, I.; Eryu, O. Characterization of femtosecond-laser-induced periodic structures on SiC substrates. *Jpn. J. Appl. Phys.* **2018**, *57*, 025602. [[CrossRef](#)]
- Yuan, Y.; Li, D.; Han, W.; Zhao, K.; Chen, J. Adjustment of Surface Morphologies of Subwavelength-Rippled Structures on Titanium Using Femtosecond Lasers: The Role of Incubation. *Appl. Sci.* **2019**, *9*, 3401. [[CrossRef](#)]
- Li, J.; Li, G.; Hu, Y.; Zhang, C.; Li, X.; Chu, J.; Huang, W. Selective display of multiple patterns encoded with different oriented ripples using femtosecond laser. *Opt. Laser Technol.* **2015**, *71*, 85–88. [[CrossRef](#)]
- Sobolewski, R.; Shi, L.; Gong, T.; Xiong, W.; Weng, X.; Kostoulas, Y.; Fauchet, P.M. Femtosecond Optical Response of Y-Ba-Cu-O Films and Their Applications in Optoelectronics. In Proceedings of the High-Temperature Superconducting Detectors: Bolometric and Nonbolometric; International Society for Optics and Photonics, Los Angeles, CA, USA, 20 May 1994; pp. 110–120.
- Liao, Y.; Cheng, Y. Femtosecond laser 3D fabrication in porous glass for micro-and nanofluidic applications. *Micromachines* **2014**, *5*, 1106–1134. [[CrossRef](#)]
- Cunha, A.; Elie, A.-M.; Plawinski, L.; Serro, A.P.; do Rego, A.M.B.; Almeida, A.; Urdaci, M.C.; Durrieu, M.-C.; Vilar, R. Femtosecond laser surface texturing of titanium as a method to reduce the adhesion of *Staphylococcus aureus* and biofilm formation. *Appl. Surf. Sci.* **2016**, *360*, 485–493. [[CrossRef](#)]
- Wang, S.; Liu, Y.; Zhang, D.; Chen, S.C.; Kong, S.K.; Hu, M.; Cao, Y.; He, H. Photoactivation of Extracellular-Signal-Regulated Kinase Signaling in Target Cells by Femtosecond Laser. *Laser Photonics Rev.* **2018**, *12*, 1700137. [[CrossRef](#)]
- Lin, C.; Cheng, C.-W.; Ou, K. Micro/nano-structuring of medical stainless steel using femtosecond laser pulses. *Phys. Procedia* **2012**, *39*, 661–668. [[CrossRef](#)]
- Vorobyev, A.; Guo, C. Femtosecond laser surface structuring technique for making human enamel and dentin surfaces superwetting. *Appl. Phys. B* **2013**, *113*, 423–428. [[CrossRef](#)]
- Kim, J.; Kim, H.N.; Lim, K.-T.; Kim, Y.; Pandey, S.; Garg, P.; Choung, Y.-H.; Choung, P.-H.; Suh, K.-Y.; Chung, J.H. Synergistic effects of nanotopography and co-culture with endothelial cells on osteogenesis of mesenchymal stem cells. *Biomaterials* **2013**, *34*, 7257–7268. [[CrossRef](#)]
- Park, S.H.; Hong, J.W.; Shin, J.H.; Yang, D.-Y. Quantitatively controlled fabrication of uniaxially aligned nanofibrous scaffold for cell adhesion. *J. Nanomater.* **2011**, *2011*, 1–9. [[CrossRef](#)]
- Zhou, P.; Mao, F.; He, F.; Han, Y.; Li, H.; Chen, J.; Wei, S. Screening the optimal hierarchical micro/nano pattern design for the neck and body surface of titanium implants. *Colloids Surf. B Biointerfaces* **2019**, *178*, 515–524. [[CrossRef](#)]
- Srivas, P.K.; Kapat, K.; Das, B.; Pal, P.; Ray, P.G.; Dhara, S. Hierarchical surface morphology on Ti6Al4V via patterning and hydrothermal treatment towards improving cellular response. *Appl. Surf. Sci.* **2019**, *478*, 806–817. [[CrossRef](#)]
- Deka, A.; Barman, P.; Bhattacharjee, G.; Bhattacharyya, S. Evolution of ion-induced nano-dot patterns on silicon surface in presence of seeding materials. *Appl. Surf. Sci.* **2020**, *526*, 146645. [[CrossRef](#)]
- Hu, J.; Hardy, C.; Chen, C.-M.; Yang, S.; Voloshin, A.S.; Liu, Y. Enhanced cell adhesion and alignment on micro-wavy patterned surfaces. *PLoS ONE* **2014**, *9*, e104502. [[CrossRef](#)]
- Martínez-Calderón, M.; Martín-Palma, R.J.; Rodríguez, A.; Gómez-Aranzadi, M.; García-Ruiz, J.P.; Olaizola, S.M.; Manso-Silván, M. Biomimetic hierarchical micro/nano texturing of TiAlV alloys by femtosecond laser processing for the control of cell adhesion and migration. *Phys. Rev. Mater.* **2020**, *4*, 056008. [[CrossRef](#)]
- Tiainen, L.; Abreu, P.; Buciumeanu, M.; Silva, F.; Gasik, M.; Guerrero, R.S.; Carvalho, O. Novel laser surface texturing for improved primary stability of titanium implants. *J. Mech. Behav. Biomed. Mater.* **2019**, *98*, 26–39. [[CrossRef](#)]
- Yasumaru, N.; Sentoku, E.; Kiuchi, J. Formation of organic layer on femtosecond laser-induced periodic surface structures. *Appl. Surf. Sci.* **2017**, *404*, 267–272. [[CrossRef](#)]
- Zwahr, C.; Welle, A.; Weingärtner, T.; Heinemann, C.; Kruppke, B.; Gulow, N.; Holthaus, M.; Lasagni, A.F. Ultrashort pulsed laser surface patterning of titanium to improve osseointegration of dental implants. *Adv. Eng. Mater.* **2019**, *21*, 1900639. [[CrossRef](#)]
- Li, C.; Yang, Y.; Yang, L.; Shi, Z.; Yang, P.; Cheng, G. In vitro bioactivity and biocompatibility of bio-inspired ti-6al-4v alloy surfaces modified by combined laser micro/nano structuring. *Molecules* **2020**, *25*, 1494. [[CrossRef](#)] [[PubMed](#)]
- Zhang, F.; Duan, J.; Zhou, X.; Wang, C. Broadband and wide-angle antireflective subwavelength microstructures on zinc sulfide fabricated by femtosecond laser parallel multi-beam. *Opt. Express* **2018**, *26*, 34016–34030. [[CrossRef](#)]
- Han, W.; Liu, F.; Yuan, Y.; Li, X.; Wang, Q.; Wang, S.; Jiang, L. Femtosecond laser induced concentric semi-circular periodic surface structures on silicon based on the quasi-plasmonic annular nanostructure. *Nanotechnology* **2018**, *29*, 305301. [[CrossRef](#)]
- Wang, S.; Jiang, L.; Han, W.; Liu, W.; Hu, J.; Wang, S.; Lu, Y. Controllable formation of laser-induced periodic surface structures on ZnO film by temporally shaped femtosecond laser scanning. *Opt. Lett.* **2020**, *45*, 2411–2414. [[CrossRef](#)]

28. Liang, Q.; Zhong, Y.; Fan, Z.; Diao, H.; Jukna, V.; Chen, W.; Houard, A.; Zeng, Z.; Li, R.; Liu, Y. Optical transmission during mid-infrared femtosecond laser pulses ablation of fused silica. *Appl. Surf. Sci.* **2019**, *471*, 506–515. [[CrossRef](#)]
29. Shi, X.; Xu, X. Laser fluence dependence of ripple formation on fused silica by femtosecond laser irradiation. *Appl. Phys. A* **2019**, *125*, 256. [[CrossRef](#)]
30. Yuan, Y.; Chen, J. Grating-assisted fabrication of sub-wavelength ripples during femtosecond laser processing of dielectrics. *Chin. Opt. Lett.* **2016**, *14*, 011404. [[CrossRef](#)]
31. Young, J.F.; Preston, J.; Van Driel, H.; Sipe, J. Laser-induced periodic surface structure. II. Experiments on Ge, Si, Al, and brass. *Phys. Rev. B* **1983**, *27*, 1155. [[CrossRef](#)]
32. Sipe, J.; Young, J.F.; Preston, J.; Van Driel, H. Laser-induced periodic surface structure. I. Theory. *Phys. Rev. B* **1983**, *27*, 1141. [[CrossRef](#)]
33. Gemini, L.; Hashida, M.; Shimizu, M.; Miyasaka, Y.; Inoue, S.; Tokita, S.; Limpouch, J.; Mocek, T.; Sakabe, S. Metal-like self-organization of periodic nanostructures on silicon and silicon carbide under femtosecond laser pulses. *J. Appl. Phys.* **2013**, *114*, 194903. [[CrossRef](#)]
34. Li, F.; Schellekens, M.; de Bont, J.; Peters, R.; Overbeek, A.; Leermakers, F.A.; Tuinier, R. Self-Assembled Structures of PMAA-PMMA Block Copolymers: Synthesis, Characterization, and Self-Consistent Field Computations. *Macromolecules* **2015**, *48*, 1194–1203. [[CrossRef](#)]
35. Le Harzic, R.; Dörr, D.; Sauer, D.; Stracke, F.; Zimmermann, H. Generation of high spatial frequency ripples on silicon under ultrashort laser pulses irradiation. *Appl. Phys. Lett.* **2011**, *98*, 211905. [[CrossRef](#)]
36. Dong, Y.; Molian, P. Coulomb explosion-induced formation of highly oriented nanoparticles on thin films of 3C-SiC by the femtosecond pulsed laser. *Appl. Phys. Lett.* **2004**, *84*, 10–12. [[CrossRef](#)]
37. Yuan, Y.; Jiang, L.; Li, X.; Wang, C.; Xiao, H.; Lu, Y.; Tsai, H. Formation mechanisms of sub-wavelength ripples during femtosecond laser pulse train processing of dielectrics. *J. Phys. D Appl. Phys.* **2012**, *45*, 175301. [[CrossRef](#)]
38. Huang, M.; Zhao, F.; Cheng, Y.; Xu, N.; Xu, Z. Origin of laser-induced near-subwavelength ripples: Interference between surface plasmons and incident laser. *ACS nano* **2009**, *3*, 4062–4070. [[CrossRef](#)]
39. Wang, J.; Guo, C. Formation of extraordinarily uniform periodic structures on metals induced by femtosecond laser pulses. *J. Appl. Phys.* **2006**, *100*, 023511. [[CrossRef](#)]
40. Yuan, Y.; Jiang, L.; Li, X.; Wang, C.; Lu, Y. Adjustment of ablation shapes and subwavelength ripples based on electron dynamics control by designing femtosecond laser pulse trains. *J. Appl. Phys.* **2012**, *112*, 103103. [[CrossRef](#)]
41. Lou, K.; Qian, J.; Shen, D.; Wang, H.; Ding, T.; Wang, G.; Dai, Y.; Zhao, Q.-Z. Recording, erasing, and rewriting of ripples on metal surfaces by ultrashort laser pulses. *Opt. Lett.* **2018**, *43*, 1778–1781. [[CrossRef](#)] [[PubMed](#)]
42. Gräf, S.; Kunz, C.; Engel, S.; Derrien, T.J.-Y.; Müller, F.A. Femtosecond laser-induced periodic surface structures on fused silica: The impact of the initial substrate temperature. *Materials* **2018**, *11*, 1340. [[CrossRef](#)]
43. Lin, X.; Li, X.; Zhang, Y.; Xie, C.; Liu, K.; Zhou, Q. Periodic structures on germanium induced by high repetition rate femtosecond laser. *Opt. Laser Technol.* **2018**, *101*, 291–297. [[CrossRef](#)]
44. Fraggelakis, F.; Stratakis, E.; Loukakos, P. Control of periodic surface structures on silicon by combined temporal and polarization shaping of femtosecond laser pulses. *Appl. Surf. Sci.* **2018**, *444*, 154–160. [[CrossRef](#)]
45. Garcell, E.M.; Guo, C. Polarization-controlled microgroove arrays induced by femtosecond laser pulses. *J. Appl. Phys.* **2018**, *123*, 213103. [[CrossRef](#)]
46. Giannuzzi, G.; Gaudiuso, C.; Di Franco, C.; Scamarcio, G.; Lugarà, P.M.; Ancona, A. Large area laser-induced periodic surface structures on steel by bursts of femtosecond pulses with picosecond delays. *Opt. Lasers Eng.* **2019**, *114*, 15–21. [[CrossRef](#)]
47. Han, W.; Han, Z.; Yuan, Y.; Wang, S.; Li, X.; Liu, F. Continuous control of microlens morphology on Si based on the polarization-dependent femtosecond laser induced periodic surface structures modulation. *Opt. Laser Technol.* **2019**, *119*, 105629. [[CrossRef](#)]
48. Yin, K.; Chu, D.; Dong, X.; Wang, C.; Duan, J.-A.; He, J. Femtosecond laser induced robust periodic nanoripple structured mesh for highly efficient oil–water separation. *Nanoscale* **2017**, *9*, 14229–14235. [[CrossRef](#)]
49. Hu, Y.; Yue, H.; Duan, J.A.; Wang, C.; Zhou, J.; Lu, Y.; Yin, K.; Dong, X.; Su, W.; Sun, X. Experimental research of laser-induced periodic surface structures in a typical liquid by a femtosecond laser. *Chin. Opt. Lett.* **2017**, *15*, 021404.
50. Han, W.; Jiang, L.; Li, X.; Liu, P.; Xu, L.; Lu, Y. Continuous modulations of femtosecond laser-induced periodic surface structures and scanned line-widths on silicon by polarization changes. *Opt. Express* **2013**, *21*, 15505–15513. [[CrossRef](#)]